Received: 22 November 2022 | Revised: 13 February 2023 | Accepted: 24 February 2023

DOI: 10.1002/rcm.9497

RESEARCH ARTICLE

Rapid Communications in Mass Spectrometry WILEY

A novel dynamic proteomics approach for the measurement of broiler chicken protein fractional synthesis rate

Jorge Peinado-Izaguerri[1,2] | Eduardo Zarzuela[3] | Mark McLaughlin[1] | Alexandra C. Small[1] | Francesca Riva[1,4] | Dorothy E. F. McKeegan[1] | Maureen Bain[1] | Javier Muñoz[3,5] | Mangesh Bhide[2] | Tom Preston[1]

[1]University of Glasgow, Glasgow, UK

[2]University of Veterinary Medicine and Pharmacy in Košice, Košice, Slovakia

[3]Proteomics Unit, Spanish National Cancer Research Center, Madrid, Spain

[4]University of Zagreb, Zagreb, Croatia

[5]Cell Signalling and Clinical Proteomics Group, Biocruces Bizkaia Health Research Institute, Biocruces Bizkaia, Barakaldo, Spain

Correspondence
Jorge Peinado-Izaguerri, University of Glasgow, Glasgow, UK.
Email: jorge.peinado@glasgow.ac.uk

Present address
Javier Muñoz, Ikerbasque, Basque Foundation for Science, Bilbao, Spain.

Funding information
European Proteomics Infrastructure Consortium providing access, Grant/Award Number: 823839; Marie Sklodowska-Curie Actions, Grant/Award Number: 765423

Rationale: The study of protein synthesis in farm animals is uncommon despite its potential to increase knowledge about metabolism and discover new biomarkers of health and growth status. The present study describes a novel dynamic proteomics approach for the measurement of protein fractional synthesis rate (FSR) in broiler chickens.

Methods: Chickens received a 10 g/kg oral dose of $^{2}H_2O$ at day 21 of their life. Body water ^{2}H abundance was measured in plasma samples using a portable Fourier transform infrared spectrometer. Free and protein-bound amino acids (AAs) were isolated and had their ^{2}H enrichment measured by gas chromatography with mass spectrometry (GC/MS). Peptide ^{2}H enrichment was measured by proteomics analysis of plasma and muscle samples. Albumin, fibrinogen and muscle protein FSR were calculated from GC/MS and proteomics data.

Results: Ala appeared to be more enriched at the site of protein synthesis than in the AA free pools. Glu was found to be the AA closest to isotopic equilibrium between the different AA pools. Glu was used as an anchor to calculate *n*(AA) values necessary for chicken protein FSR calculation in dynamic proteomics studies. FSR values calculated using proteomics data and GC/MS data showed good agreement as evidenced by a Bland–Altman residual plot.

Conclusions: A new dynamic proteomics approach for the measurement of broiler chicken individual protein FSR based on the administration of a single $^{2}H_2O$ oral bolus has been developed and validated. The proposed approach could facilitate new immunological and nutritional studies on free-living animals.

1 | INTRODUCTION

Protein turnover is critical for the maintenance of all cellular processes and its disruption is associated with a wide range of disorders, including cardiac and neurodegenerative diseases and reduced growth.[1–3] Although neglected for some time, its study is now understood to be an essential part of systems biology approaches that aim to understand whole-cell proteostasis, as mRNA expression usually correlates poorly with net protein concentration.[4–6] The study of protein synthesis is also extremely valuable from a biomarker discovery perspective due to the fact that protein synthesis rates change rapidly in advance of measurable changes in protein concentration.[7] Moreover, the study of protein turnover could reveal alterations in protein metabolism which would

not result in an alteration of protein concentration, and therefore could not be unravelled by static measurements of protein concentration, which is determined by the balance between protein synthesis and degradation. Despite of the importance of studying protein synthesis, little work has been performed in the area related to farm animals.

Lack of studies concerning protein synthesis is surprising in the case of broiler chickens. Chickens can be regarded as a genetic and physiological model system for the study of muscle growth.[4] Moreover, poultry meat is currently the biggest meat industry segment and global meat production is expected to reach 377 Mt by 2031.[8] Studies of chicken protein dynamics have been mostly limited to mixed muscle protein (MMP) turnover and mixed liver protein turnover to a lesser degree.[9–23] Notable exceptions to this trend are the work of Barnes et al[24] and Doherty et al.[25] The Barnes et al study reported hemopexin fractional synthesis rate (FSR) during an immune challenge, in addition to mixed muscle and liver protein synthesis, being the first and only measurements of a chicken acute phase protein FSR, while the study of Doherty et al reported individual sarcoplasmic protein turnover rate. Further investigation of broiler chicken individual protein synthesis rate could expand our current knowledge regarding broiler chicken growth and immune function, especially as protein and amino acid (AA) metabolism in chickens is intimately related with these metabolic events.[26]

Most common strategies for the study of protein synthesis aim to measure the incorporation of an isotopically labelled precursor into the protein product. Studies of chicken protein synthesis have been mostly limited to the use of radioactively labelled AAs first and AAs labelled with stable isotopes later, these AAs (predominantly Phe and Tyr) being administered intravenously or added to the chicken diet.[9,11,12,15–17,27] The method involving the intravenous administration of a flooding dose of ^{15}N-Phe followed by the assessment of AA isotopic enrichment by gas chromatography with mass spectrometry (GC/MS) seems to have become the gold standard in the field with all studies of broiler protein synthesis in the last decade having adopted it.[19–23,28,29] These methods have been associated with several problems such as difficulties in assessing the true precursor enrichment at the site of synthesis (aminoacyl t-RNAs), the necessity of confined conditions and the high cost of AA tracers.[30] The use of deuterated water (^2H_2O) as tracer eliminates most of these problems as it is a safe and inexpensive tracer that can be administered orally and equilibrates rapidly with body water (BW), labelling all AAs across different cellular compartments.[31–34] Studies of protein synthesis using ^2H_2O usually follow one of two labelling strategies. The most common protocol administers a loading dose of ^2H_2O, often followed by a series of 'top-up' ^2H_2O doses added to drinking water. The aim being to calculate protein FSR by measuring deuterium (^2H) enrichment in the product over a pseudo-linear increase phase following ^2H_2O administration.[35,36] When continued over the longer term, this strategy more obviously aims to increase BW ^2H enrichment to a plateau level maintained over time and always requires subsequent ^2H_2O inputs following the initial dose.[35,37] FSR is calculated by fitting measured product ^2H enrichment to the theoretical exponential rise in enrichment (see Equation 1 below). Early studies measured product ^2H enrichment in protein-bound AAs, usually by GC/MS, which limited protein FSR calculation to isolated proteins or mixed tissue protein.[34,38] As the field progressed, the combination of ^2H_2O labelling with the use of proteomics liquid chromatography (LC)/MS/MS platforms for the measurement of peptide ^2H enrichment gave birth to dynamic proteomics studies capable of measuring individual protein FSR within complex protein mixtures.[39,40]

An alternative labelling strategy was proposed which makes use of a single-bolus dose of ^2H_2O for the calculation of protein FSR over the period that deuterium oxide eliminates from the body (elimination half-time of *ca* 7 days in adult humans; *ca* 2 days in chicken).[41–43] This approach was informed by the single exponential tracer elimination kinetics established through experience of the doubly labelled water method to measure total energy expenditure.[44] This methodology further increases the convenience of ^2H_2O labelling and it is also beneficial from an economic perspective as a lower amount of tracer can be used. In this bolus tracer approach, FSR is calculated by curve fit to a modified exponential model (Equation 4, below). This approach could be especially appropriate for the study of protein synthesis in free-living farm animals over the medium term. It would be difficult to maintain steady ^2H BW labelling as, unlike with humans, it is difficult to time the ingestion of repeated doses while the addition of ^2H_2O to drinking water would usually translate in significant economic losses due to water spillage and further dosing difficulties in animals that were not housed or in animals that were housed together.

The study presented here aimed to develop a novel approach, based on a single ^2H_2O oral bolus, to study individual protein FSR by dynamic proteomics in broiler chickens. The secondary objective was to check a number of underlying assumptions related to the use of ^2H_2O as an isotopic tracer in the broiler chicken as well as to define some of the parameters needed for FSR calculation. Plasma free, muscle free and liver free AA ^2H enrichment is reported in addition to albumin-bound, fibrinogen-bound and MMP-bound AA ^2H enrichment. This then allows a 'conventional' calculation of protein FSR from bound-AA enrichment in isolated proteins (or bulk tissue protein) as product. The proposed dynamic proteomics approach for estimating FSR was applied and validated by comparison with a GC/MS approach.

2 | MATERIALS AND METHODS

2.1 | Experimental design and *in vivo* animal procedures

All chemicals were supplied by Sigma-Aldrich (Gillingham, UK) unless otherwise stated.

A total of 140, one-day-old, male Ross 308 broiler chicks (PD Hook Hatcheries Ltd, UK) were part of two different animal trials

held in June and August 2019 at the University of Glasgow Cochno Farm and Research Centre. The first trial comprised two experimental groups ('Challenged' and 'Unchallenged') while the second trial comprised three experimental groups ('Control Diet', 'Diet 1' and 'Diet 2'). Each experimental group comprised 28 chicks randomly housed in groups of 7 across four replicate 2.5 m^2 pens on a litter of wood shavings. Table S1 summarizes the differences between experimental groups. Access to feed and water was available *ad libitum* over the entirety of the trials. Chicken starter (provided from day 1 to 14) and grower (provided from day 14 onwards) corn-soybean meal-based basal diets were designed in collaboration with the company Nuscience (Ghent, Belgium). Details of the composition of these diets can be found in Table S2. The quantity of nutrients provided by the formulated diets was slightly suboptimal in comparison with commercially available diets (approximately 97% recommended energy and digestible AA requirements). Birds that were part of the experimental groups Diet 1 and Diet 2 received a modified version of the standard diet which contained a lemon-derived feed additive (300 g/ton) and a cucumber-derived feed additive (75 g/ton), respectively. Room temperature was set at 30°C at the start of the trial and decreased 1°C each three days to a final temperature of 23°C at the end of the experiment (day 25), as recommended in the Ross 308 breeder management guide (Aviagen, Midlothian, UK). A 23 h:1 h light:dark cycle was implemented from day 1 to day 12, this cycle being changed to 18 h:6 h light:dark from day 12 onwards. Broilers were weighed twice a week from the start of the trial and climatized to handling by the start of the experiment. All animal procedures were conducted under UK Home Office licence (no. P4A4CA831) and approved by the University of Glasgow MVLS College Ethics Committee.

Experiments started on day 21 of each chicken's life (0 h) when five birds per pen were administered an oral dose of ^2H_2O (10 g/kg 99.8 atom percent ^2H_2O), which was dropped into the bird's beak while its movement was restrained, using a 10 mL syringe. The ^2H_2O dose volume aimed to raise BW ^2H enrichment to > ~ 1% APE (atom percent excess). At 1 h after ^2H_2O administration all birds received a subcutaneous injection of *Escherichia coli* lipopolysaccharide (from *E. coli* O111:B4; 2 mg/mL) where the volume in mL was equal to the bird's body weight in kg (for a final 2 mg/kg of body weight). Birds from the Unchallenged experimental group were injected an equal volume of sterile saline (0.9% sodium chloride). One ^2H_2O-dosed bird from each pen was blood sampled and culled at 4, 24 and 48 h timepoints while two dosed birds were blood sampled and culled at 96 h. The two undosed birds from each pen were blood sampled and culled at 48 and 96 h. All chickens were culled by an overdose (1.5–2 mL) intravenous injection of barbiturate (Euthatal 200 mg/mL, Merial, UK).

Blood samples were collected from a wing vein using a syringe and transferred into EDTA-coated tubes (Midmeds, Hertford, UK) and their volume ranged between 1.5 and 2 mL. Blood tubes were centrifuged (3000*g*) for 15 min at 4°C, and plasma was collected, aliquoted and immediately frozen at −20°C. Samples from different organs were collected from all chickens including breast muscle and liver. All samples were snap-frozen at −80°C using a dry ice bath. At the end of each day, plasma and tissue samples were transferred to a −80°C freezer.

2.2 | Plasma Fourier transform infrared analysis

BW ^2H abundance was directly measured from thawed plasma samples using a portable Fourier transform infrared (FTIR) spectroscopy instrument (model 4500, Agilent, Cheadle, UK) by measuring the absorbance of D–O bonds around a wavenumber of 2504 cm^{-1}. FTIR spectroscopy has been applied previously for the measurement of ^2H abundance in saliva.[45] The use of the Agilent 4500 portable FTIR instrument with DialPath transmission interface for the measurement of ^2H abundance in saliva and plasma had been validated in our laboratory by comparing its accuracy with that of an isotope ratio mass spectrometer (HYDRA 20–22, SerCon, Crewe, UK; unpublished). Optimal resolution for this application was found to be 8 cm^{-1}. A 100 µm optical pathlength and a 3 h instrument warm-up time were used.

All plasma samples collected over the course of our experiments had their ^2H abundance measured. Two water standards (0 and 1000 mg/kg excess deuterium) were measured at the beginning and end of each sample batch. All measurements (samples and standards) were made in duplicate by pipetting a volume of 20 µL of plasma onto the optical window. BW ^2H abundance data were calculated using an internal calibration model and exported from the manufacturer's Microlab software and subsequent data analysis was performed in Microsoft Excel.

For the determination of BW ^2H enrichment, duplicate measurements of ^2H abundance (mg/kg) were first averaged and then corrected by comparison with ^2H abundance measured in the standards, the protein content of plasma samples (assumed to be 4.5% in chicken) and the dilution factor resulting from the dead volume remaining in the dosing syringes after ^2H_2O administration (determined by weight difference). Measurements were transformed to molar abundance from the weight/weight calibration of the FTIR instrument. Finally, enrichment values were obtained by subtracting baseline abundance calculated for a control chicken and expressed in APE.

2.3 | Fibrinogen-bound AA purification

Fibrinogen was isolated from 0.8 mL plasma aliquots from samples collected at each experimental timepoint as well as an unlabelled sample from one pen for each of the three experimental groups in our second experiment, for a total of 15 samples. The isolation method was adapted from the work of Takeda.[46] A plasma volume of 800 µL was mixed with an equal volume of 0.09 M sodium citrate and 533 µL of 4 M $(NH_4)_2SO_4$, left to rest at room temperature for 5 min and spun for 5 min at 1000*g* to form a pellet. The supernatant was discarded and the pellet was washed three times with 1600 µL of 1 M

$(NH_4)_2SO_4$, resuspended in 600 µL of 0.005 M sodium citrate, reprecipitated with 200 µL of 4 M $(NH_4)_2SO_4$, washed again with 1600 µL of 1 M $(NH_4)_2SO_4$ once and resuspended in 160 µL of 0.005 M sodium citrate. This fibrinogen solution was then refrigerated for 1 h at 4°C and re-spun if a precipitate was observed.

The fibrinogen solution had 300 nmol of norvaline internal standard (30 µL of 10mM) added before being freeze-dried. Glass vials containing the fibrinogen pellet had 200 µL of 6 M HCL added and were placed in a PTFE hydrolysis vessel, where an additional volume of 6 M HCL to a maximum volume of 5 mL was added to the vessel. Oxygen was excluded by gassing nitrogen into the vessel for 10 min before the vessel was quickly capped with its PTFE seal and enclosed within a stainless steel pressure vessel (model 4748, Parr, Moline, USA). Samples were hydrolysed in a programmed temperature oven at 150°C for 4 h.

2.4 | Albumin-bound and plasma free AA purification

Albumin-bound and plasma free AAs were obtained from plasma samples collected at each experimental timepoint as well as an unlabelled sample for one pen from each of our experimental groups for a total of 25 samples. Plasma free AAs were separated from plasma protein content following a trichloroacetic acid (TCA) precipitation in the presence of a reducing agent as described by Svagera et al.[47] A plasma volume of 800 µL was mixed with 200 µL of carbonate buffer (5mM Na_2CO_3) containing norvaline internal standard (240 nmol), 200 µL of 0.5% tris(hydroxypropyl)phosphine and 800 µL of 10% TCA before being spun for 10 min at 1000*g*. The resulting supernatant containing acidified plasma free AAs was poured directly onto a cation-exchange column and diluted to 10 mL with deionized water.

The plasma protein pellet was resuspended in 800 µL of 10% TCA, washed and spun twice before being resuspended again and refrigerated at 4°C for 1 h, with supernatants being discarded. The plasma protein suspension was then spun and the resulting pellet had 2 mL of 95% ethanol added in order to solubilize its albumin content as reported by Korner and Debro.[48] The mixture was centrifuged for 10 min at 1000*g* and its supernatant containing purified albumin was aspirated. An amount of 200 µL of albumin-containing supernatant had 30 µL of norvaline internal standard (10mM) added before being freeze-dried prior to acid hydrolysis as previously described.

2.5 | Muscle protein-bound, muscle free and liver free AA purification

The 25 muscle and liver samples from which AAs were obtained were collected from the same birds from which the plasma samples utilized for albumin isolation were collected. An amount of 200 mg of tissue was mixed with a volume of 0.3 M NaOH (1 mL for liver samples and 1.5 mL for muscle samples) and 30 µL of norvaline internal standard (10mM) was added. The resulting mixture was homogenized manually using a glass rod before being incubated at 40°C for 1 h. The tissue mixture was spun for 5 min at 1000*g* and the resulting supernatant decanted into a new tube where 2 mL of 10% TCA was added before being refrigerated at 4°C for 1 h and spun for 10 min at 1000*g*. The resulting supernatant containing acidified muscle free AAs or liver free AAs was poured directly into a cation-exchange column and diluted to 10 mL with deionized water.

Liver protein pellets were discarded while muscle protein pellets were washed twice with 1 mL of 10% TCA before 30 µL of norvaline internal standard (10mM) was added. The pellets were then freeze-dried and acid-hydrolysed as previously described.

2.6 | AA purification and derivatization

AA samples resulting from protein acid hydrolysis were resuspended with 5 mL of deionised water. All AA samples were loaded into 10 mL poly-Prep columns (Bio-Rad, Watford, UK) with a 2 mL bed volume of Dowex 50W-X8 100–200 mesh cation-exchange resin, mounted on a solid-phase extraction manifold. The columns were washed to waste with 10 mL of deionized water and AAs were eluted into 10 mL glass tubes with a volume of 5 mL of 4 M NH_4OH followed by 2 mL of deionized water. AA samples were vacuum-dried at 65°C for 7.5 h.

AAs were derivatized as ethoxy carbonyl ethyl esters following the modifications of Svagera and co-workers.[47,49] Briefly, 600 µL (1.2 mL for protein-bound AA samples) of aqueous solvent (60:32:8, deionized water/ethanol/pyridine) was added to the dry sample and agitated before resting for 5 min. AAs were derivatized with 600 µL of a combined organic extraction solvent (1.2 mL for protein-bound AA samples) (10:6:1, isooctane/butyl acetate/ethyl chloroformate). This was mixed with the aqueous AA solution and left to rest for 5 min before being spun for 10 min at 1000*g*. A volume of 400 µL was aspirated from the upper phase and placed into a tapered GC vial along with *ca* 20 mg of anhydrous granular Na_2SO_4 as desiccant.

2.7 | AA GC/MS analysis

The deuterium enrichment in free and bound AAs was measured by GC/MS, using a model 5977C (Agilent, Cheadle, UK). The GC system was fitted with a 20 m × 0.18 mm ID × 0.36 µm film column with a 5 m retention gap (Rxi-5Sil MS, Thames Restek, UK). Samples (1 µL) of the derivatized AAs were injected in splitless mode into an inert glass liner held at 280°C. The column oven temperature programme started at 80°C, being held for 1.5 min before being ramped at 8°C/min to 320°C and held for 0.5 min. The carrier gas was helium and the flow rate was constant at 0.7 mL/min.

The MS ion source was operated in electron ionization mode with a selected ion monitoring sequence of eight groups. The masses monitored conformed to the base peak as reported in the literature for this derivative.[50] In each case the base peak (M^+) and M + 1 peak

were monitored. Higher masses were not monitored as the application uses relatively low enrichments so that the chance of an AA containing more than one deuterium atom is minimal. In the case of Phe, two fragment ion groups were monitored. Ions at 176 Da (and 177 Da) and 91 Da (and 92 Da) were monitored to confirm that the mechanism of labelling indispensable AAs involved exchange of a single H atom at C2, which is contained in the 176 Da fragment but not in the 91 Da fragment. Use of eight selected ion monitoring groups maintained sensitivity by allowing a small number of masses to be monitored in each group, while detector gain could be optimized in each group.

The manufacturer's Masshunter software was used to integrate peak area response and to export all data to an Excel spreadsheet. ^{2}H enrichment was calculated for each AA and was expressed in units of mole % excess (MPE).

2.8 | Sodium dodecylsulfate–polyacrylamide gel electrophoresis (SDS-PAGE)

Five chicken plasma samples were used to check the purity of isolated albumin and fibrinogen. Albumin was purified from three samples while fibrinogen was purified from two samples. An amount of 10 µg of protein was denatured at 95°C for 4 min in 4× Laemmli buffer and 1 M dithiothreitol (DTT). Samples were loaded into a Criterion XT precast gel of 4–12% Bis-Tris (Bio-Rad, Watford, UK). The gel was run at 145 V for 1.5 h in XT-MES running buffer (Bio-Rad, Watford, UK), stained with Coomassie Brilliant Blue R-250 and destained with destaining solution (10/50/40, acetic acid/methanol/deionized water). Gel images were taken using a Bio-Rad ChemiDoc XRS instrument (Bio-Rad, Watford, UK).

2.9 | Muscle protein extraction for proteomics

Protein content was extracted for proteomics analysis from the same muscle samples from which muscle free and protein-bound AAs were extracted, except for the samples collected at the 4 h timepoint, for a total of 20 samples. Protein extraction procedure was adapted from the work of Almeida and co-workers.[51] An amount of 200 mg of tissue was mixed with 1 mL of 50mM ammonium bicarbonate, 8 M urea, 2 M thiourea and 10 µL of Halt™ protease inhibitor cocktail (100×) (Thermo Fisher Scientific, Renfrew, UK). A 5 mm diameter stainless steel milling ball was added to the tube. The mixture was homogenized using a Retsch MM400 oscillating mill (Retsch GmbH, Haan, Germany) for 2 min at 30 Hz. Samples were spun for 6 min at 12 500*g* and the resulting supernatant was collected. An amount of 100 µL of the collected supernatant was mixed with 900 µL of SDS buffer (4% SDS, 100mM Tris/HCL (pH 8.2), 0.1 M DTT), heated for 5 min at 95°C and placed for 10 min in an ultrasonic bath (U100, Ultrawave, Cardiff, UK). Protein content was assessed using a Pierce 660 nm protein assay kit (Thermo Fisher Scientific, Renfrew, UK).

2.10 | LC/MS/MS data acquisition and isotopologue abundance extraction

Twenty-five plasma aliquots of the samples from which plasma free AAs and albumin-bound AAs were purified and the 20 protein extracts obtained from muscle samples were analysed by LC/MS/MS using an UltiMate 3000 RSLnano LC system coupled to either a Q Exactive HF-X (muscle samples) or a Q Exactive HF (plasma samples) mass spectrometer equipped with an EASY-Spray source (Thermo Fisher Scientific, Renfrew, UK). Samples (50 µg protein content) were solubilized in 2% SDS and 100mM triethylammonium bicarbonate (pH 7.55). Proteins were reduced and alkylated (15mM tris(2-carboxyethyl)phosphine, 25mM chloroacetamide) at 45°C for 60 min. Then, proteins were digested with trypsin (Promega, Wisconsin, USA) and Lys-C (Wako, Osaka, Japan) (protein:enzyme ratio 1:50, 16 h at 37°C) using a single-tube, solid-phase-enhanced sample preparation method.[52] Peptides were loaded into an Acclaim PepMap 100 C18 LC column (5 µm particle size, 100 µm diameter, 20 mm length) (Thermo Fisher Scientific, Renfrew, UK) followed by an EASY-Spray PepMap RSLC C18 column (2 µm particle size, 75 µm diameter, 500 mm length) (Thermo Fisher Scientific, Renfrew, UK) operated at 45°C and separated using a 60 min effective gradient (buffer A: 0.1% formic acid; buffer B: 100% acetonitrile, 0.1% formic acid) at a flow rate of 250 nL/min. The gradient used was: from 2% to 6% of buffer B in 2 min, from 6% to 33% B in 58 min, from 33% to 45% B in 2 min, plus an additional 10 min at 98% B. Peptides were sprayed at 1.5 kV into the mass spectrometer and the capillary temperature was set to 300°C. The mass spectrometer was operated in a data-dependent mode with the top 12 (muscle samples) or top 10 (plasma samples) ions being selected for fragmentation. Intensity threshold was either ≥3.5e5 (muscle samples) or ≥2.2e4 (plasma samples) and charges +1 and > +6 were excluded. Mass spectra were acquired from 350 to 1400 *m/z* with a resolution of 60 000 FWHM (200 *m/z*).

Fifteen plasma aliquots of the samples from which fibrinogen was purified were also analysed by LC/MS/MS using an Acquity M-class nano LC system coupled to a Synapt G2Si mass spectrometer equipped with a nanospray source (Waters, Prague, Czech Republic). Plasma was precipitated with 9 volumes of ice-cold acetone overnight, centrifuged and the resulting pellet dissolved in 8 M urea. Samples (100 µg protein content) were reduced (10mM DTT, 100mM ammonium bicarbonate) at 37°C for 60 min. Alkylation (50mM iodoacetamide, 100mM ammonium bicarbonate) was performed in the dark for 30 min. Then, proteins were digested with trypsin (Promega, Wisconsin, USA) (protein:enzyme ratio 1:100, 16 h at 37°C). Peptides were loaded into a nanoEase MZ Symmetry C18 Trap column (5 µm particle size, 180 µm diameter, 20 mm length) (Waters, Prague, Czech Republic) followed by a nanoEase HSS T3 column (1.8 µm particle size, 75 µm diameter, 100 mm length) (Waters, Prague, Czech Republic) operated at 40°C and separated using a 115 min effective gradient (buffer A: 0.1% formic acid; buffer B: 100% acetonitrile, 0.1% formic acid) at a flow rate of 300 nL/min. The gradient used was: 5% of buffer B from 0 to 5 min, from 5% to 35% B

in 115 min, plus an additional 8 min at 85% B. Peptides were sprayed at 2.8 kV into the mass spectrometer with the source temperature being set to 80°C and the desolvation temperature being set to 220°C. The mass spectrometer was operated in a fast data-dependent mode with the top 10 ions being selected for fragmentation. Intensity threshold was ≥6000 and charges +1 and > +6 were excluded. Mass spectra were acquired from 300 to 2000 *m/z* with a resolution of 20 000 FWHM.

Protein identification from Thermo raw files was performed using MaxQuant 2.0.1.0 (Andromeda search engine) while protein identification from Waters raw files was performed using the instance of MSAmanda which is embedded in Skyline (version 21.1.0.146) (MacCoss Lab, University of Washington, USA).[53–55] Identification was performed against a *Gallus gallus* database (Swiss-Prot/TrEMBL, 34 808 sequences, accessed June 23, 2021). Cysteine carbamidomethylation was set as a fixed modification while methionine oxidation and protein N-terminal acetylation were set as variable modifications. A maximum of two missed cleavages per peptide were allowed following trypsin digestion. Peptides and proteins were filtered at 1% false discovery rate (calculated from posterior error probability scores for Thermo data and *q*-value scores for Waters data). For repeated peptides, only an instance assigned to the leading razor protein was considered for analysis.

Peptide mass isotopologue intensities were mined using Skyline. A spectral library was built by Skyline BiblioSpec tool using the results from the peptide search and proteome raw data. The number of transitions to be displayed was limited to four (M_0 to M_3). Peptides were manually selected for FSR calculation based on the consistency of their peak shape quality (Gaussian peak shape considered optimal) and absence of interfering transitions across all samples within the same batch. Six different albumin peptides were selected from the 25 plasma samples from which albumin had been purified, six different fibrinogen peptides (three corresponding to its alpha subunit, one to its beta subunit and two to its gamma subunit) were selected from the 15 plasma samples from which fibrinogen had been purified and six different myosin heavy chain (MYHC) peptides were selected from the 20 analysed muscle samples. Mass isotopologue intensity was exported from Skyline and subsequent data analysis was performed in Microsoft Excel.

Peptide ^2H abundance was calculated as described elsewhere using the following formula[37]:

$$\text{Peptide mol}\%(\text{MP}) = \text{MPM}_1 \times 1 + \text{MPM}_2 \times 2 + \text{MPM}_3 \times 3 \quad (1)$$

where MPM_i is determined as

$$\text{MPM}_i = \left[\text{M}_i / \sum(\text{M}_0 \ldots \text{M}_3)\right] \times 100\% \quad (2)$$

Similar to the rest of the ^2H enrichment calculations, peptide baseline ^2H abundance was measured for each pen undosed chicken which was subtracted from that measured at each timepoint in order to obtain peptide enrichment (MPE).

2.11 | FSR calculation

The equations used to calculate protein FSR following a single ^2H_2O bolus administration are derived from the equation (Equation 3) that has been used in many protein FSR studies, usually based on the assumption of a single compartment, which aims to fit the labelling of the product (peptide or protein-bound AAs) to an exponential growth curve[35,37,40]:

$$\text{Product labelling} = \text{asymptotic labelling} \times \left(1 - e^{-k1 \times t}\right) \quad (3)$$

This equation allows the calculation of the rate constant (k_1) by the least squares method, being preferable to have product labelling data from, at least, four different timepoints. In this study this calculation was facilitated by the SOLVER function in Microsoft Excel, which made use of peptide ^2H enrichment data from five different birds culled at 4, 24, 48 and 96 h post-^2H_2O administration as well as an undosed bird as baseline. For MMP and myosin FSR calculation, data from four different birds were used as the 4 h timepoint was excluded due to the low ^2H enrichment found in muscle samples during a pilot analysis (data not shown). This decision had the objective to maximize economic and time efficiency. It should be noted that, as a result of culling one chicken at each timepoint, calculated FSR values in this study refer to each experimental pen instead of individual birds.

Following a plateau labelling experimental design, the asymptotic product labelling represents the maximum value that the product will eventually reach and that reflects the labelling reached by the precursor pool shortly after ^2H_2O administration, which is maintained throughout the experiment. However, when a single bolus labelling approach is being applied, precursor pool labelling will steadily decline after an initial maximum value. The rate of decline in precursor labelling (k_2) is assumed to be equal in BW and free AA pools due to their fast equilibration. BW k_2 was expressed as the slope of the regression line that relates the elimination of the natural logarithm of BW ^2H enrichment with time for each individual pen.

When using a GC/MS approach for the calculation of protein FSR based on the measurement of a protein-bound AA enrichment as product and free AA enrichment as precursor, Equation (4) should be used when a plateau labelling strategy is applied while Equation (5) would be its equivalent when a single bolus labelling strategy is applied. The difference between the kinetic models is graphically represented in Figure S1.

$$B = f \times \left(1 - e^{-k1 \times t}\right) \quad (4)$$

$$B = f \times e^{k2 \times t} \times \left(1 - e^{-k1 \times t}\right) \quad (5)$$

where B is the enrichment of a protein-bound AA at a certain timepoint (t) and f is the maximum enrichment of that AA in the free pool.

A variation of Equation (4) and Equation (5) can be expressed when using measurements of BW ^{2}H enrichment as the precursor from which asymptotic product labelling can be calculated. However, as BW is not the precursor for protein synthesis, an additional factor is introduced that relates BW enrichment to AA enrichment. This describes the maximum apparent number of ^{2}H atoms that can be incorporated by each AA and is often expressed as *n*(AA). In a plateau labelling protocol this can be determined from free AA enrichment once isotopic equilibrium has been established. As the true precursor enrichment is not necessarily the same as the measured free pool enrichment, plateau labelling can be continued until fast-turnover proteins have come to isotopic equilibrium and *n*(AA) can be measured in the protein pool. To determine *n*(AA) values in a single-bolus protocol an alternative approach is required. Free AA ^{2}H enrichment measurements can be plotted against BW ^{2}H enrichment at each timepoint. The slope of this linear regression gives a measure of *n*(AA) in the particular free pool as AA labelling from BW is rapid. The following equation would then be used to estimate FSR:

$$B = p \times n(\mathrm{AA}) \times e^{k2 \times t} \times \left(1 - e^{-k1 \times t}\right) \quad (6)$$

where *p* represents the maximum ^{2}H BW enrichment expressed as the exponential of the intercept of the regression line of the natural logarithm of BW ^{2}H enrichment with time for each individual pen.

Dynamic proteomics approaches allow the measurement of peptide ^{2}H labelling (*E*), which can be used as the product for FSR calculation. The sum of the *n*(AA) values for each AA present in the peptide motif is calculated to derive an *n*(pep) value. As a result, we obtain an equation (Equation 7) that allows the calculation of FSR for each peptide from proteomics data following a single ^2H_2O bolus labelling approach:

$$E = p \times n(\mathrm{pep}) \times e^{k2 \times t} \times \left(1 - e^{-k1 \times t}\right) \quad (7)$$

Accurate *n*(pep) calculation requires a curated list of *n*(AA) values. The method previously described for the calculation of *n*(AA) does not allow a full list to be obtained because several AAs are not readily analysed following the derivatization method applied for GC/MS analysis. Additionally, it has been previously observed that free AA enrichment values may not accurately represent the enrichment of the true precursor pool for protein synthesis (aminoacyl t-RNAs). This observation had led previous studies to develop innovative methods to determine *n*(AA) from product enrichment data.[37,39,40] A novel approach appropriate for the tracer bolus design described here has been developed in order to determine an *n*(AA) list from product enrichment data.

This approach uses an anchor AA from which *n*(AA) values will be derived for other AAs. The chosen anchor AA should be as close as possible to isotopic equilibrium between the measured free AA pools as well as having a ^{2}H elimination rate (AA k_2) close to BW ^{2}H elimination rate (k_2) and to incorporate sufficient deuterium to facilitate its precise measurement. The chosen anchor AA can also be the one used for GC/MS-based FSR calculation (Equation 6). Glu was the chosen anchor AA here (details in Section 3).

The *n*(AA) values for AAs other than Glu were then obtained by multiplying *n*(Glu), determined as the slope of the regression line that relates Glu ^{2}H enrichment to BW ^{2}H enrichment, by the ratio of the enrichment of each AA to Glu in the protein-bound AA pool. The latter was obtained from the slope of the regression line that relates each AA to Glu ^{2}H enrichment through all analysed protein-bound AA samples. The underlying principle being that AA enrichment ratio in the bound pool will reflect that in the true precursor pool.

3 | RESULTS

3.1 | BW ^{2}H enrichment

Elimination plots were created by plotting BW ^{2}H enrichment (ln APE) against time for each pen in both experiments. Among the two available 96 h measurements for each pen, the one that best fitted the regression line was chosen, based on the lowest root mean square error. This action was taken to save the expense and complexity of additional AA and peptide analysis and because it had been observed that some birds regurgitated a portion of the dose which would result in lower enrichment in the free AA and protein pools in that bird. Average BW ^{2}H elimination half-time was 1.92 days in the first experiment and 2.03 days in the second experiment. Average initial BW ^{2}H enrichment was 1.26 APE in the first experiment and 1.46 APE in the second experiment. Among the four replicate pens available from each experimental group, the pen with the highest R^2 was selected for plasma, muscle and liver free AA ^{2}H enrichment analysis as well as albumin and MMP isolation and bound AA ^{2}H enrichment analysis. Pens with the second highest R^2 value from the second experiment were selected for fibrinogen isolation and bound AA ^{2}H enrichment analysis.

3.2 | Free AA ^{2}H enrichment

Aggregated free AA ^{2}H enrichment data (MPE) from 25 analysed samples corresponding to one pen per experimental group were plotted against BW ^{2}H enrichment in order to calculate *n*(AA) for different AAs for each of the free AA pools analysed (Figure 1). It should be noted that muscle free AA enrichment data appeared noisier than other datasets, probably due to the lower free AA concentration in these samples. AA ^{2}H enrichment calculated for low-enrichment/low-concentration AA was not judged adequately precise for analysis.

A comparison between calculated *n*(AA) values across the different pools (Table S3) revealed differences in AA enrichment. The difference between Ala and Leu extracellular and intracellular *n*(AA) values was notable with intracellular *n*(Ala) being 25% lower than extracellular and intracellular *n*(Leu) being almost 30% lower. Logarithmic plots of ^{2}H enrichment against time (Figure S2) showed

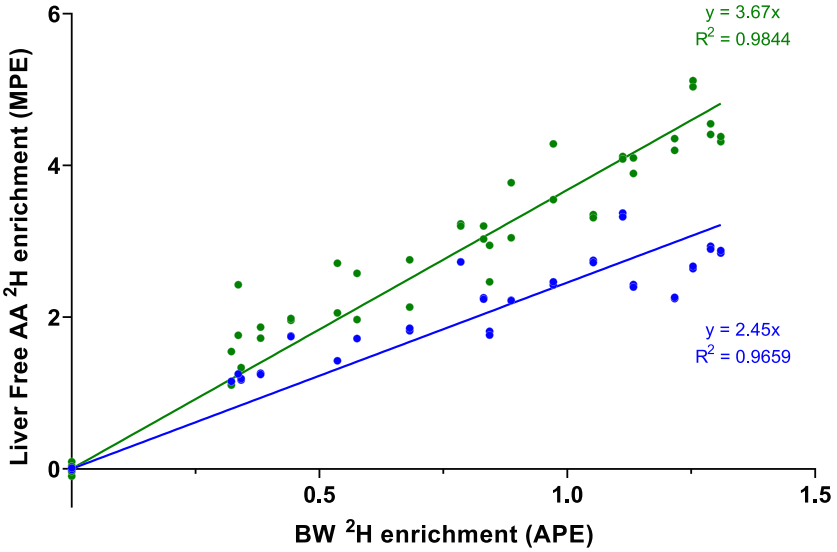

FIGURE 1 Liver free alanine (blue) and glutamate (green) ^{2}H enrichment against BW ^{2}H enrichment. Slopes of the regression lines represent liver *n*(AA) value. [Color figure can be viewed at wileyonlinelibrary.com]

that while most AAs show a similar ^{2}H elimination rate (AA k_2) compared to BW (BW k_2; $-0.013\ h^{-1}$) in the plasma free pool, differences can be observed across the intracellular free pools. Leu k_2 appeared slower than BW k_2 across both intracellular pools ($-0.008\ h^{-1}$ in muscle and $-0.002\ h^{-1}$ in liver) while Ala k_2 ($-0.007\ h^{-1}$) was slower than BW elimination in the liver free pool. Overall, results obtained from free AA ^{2}H enrichment suggest evidence for compartmentation with different AA pools having greater effect on the apparent isotopic equilibration between BW and free AA. Glu was the AA that came closest to isotopic equilibrium between the different analysed pools and showed a Glu k_2 of $-0.011\ h^{-1}$ in plasma, $-0.013\ h^{-1}$ in muscle and $-0.010\ h^{-1}$ in liver.

3.3 | Protein-bound AA ^{2}H enrichment

SDS-PAGE was used to assess the purity of albumin and fibrinogen extracts (Figure S3).[56]

It should be noted that the acid hydrolysis procedure that was applied in order to free AAs from the protein backbone, allowing the analysis of protein-bound AAs, causes the deamidation of Asn and Gln. This means that while our free AA datasets show the true enrichment of Glu and Asp, our protein-bound AA datasets combine the enrichment of Glu with Gln and Asp with Asn. Recently published literature *n*(AA) values have shown very similar ^{2}H enrichments for Glu and Gln which lead us to trust the data for these AAs.[40] However, Asp and Asn reported ^{2}H enrichment values were different enough to avoid using the aggregated Asp/Asn data collected as they would not be comparable to the free Asp or free Asn data.

It was observed that ^{2}H enrichment ratios between AAs were different across the different pools, especially when comparing free and protein-bound AA pools. An example of this observation is the relation between Glu and Ala ^{2}H enrichment across the different analysed AA pools (Figure S4). ^{2}H enrichment ratios show that Glu was more enriched than Ala in the free AA pools (as plasma free *n* (AA) had shown) while Ala seemed to be more enriched than Glu in the three protein-bound AA pools analysed in this study. This observation suggests that *n*(Ala) is higher than *n*(Glu) in the true precursor pool. Further evidence for this phenomenon can be found when looking at the ratios between these AAs and BW ^{2}H enrichment over time (Figure 2). It can be observed how albumin-bound Ala and fibrinogen-bound Ala ^{2}H enrichment ratio to BW increased beyond the values observed in all analysed free pools which indicates that *n*(Ala) at the true site of synthesis was greater than that in the analysed free pools. Contrarily, protein-bound Glu ratio increased over time until reaching similar values to those in the free analysed pools (apparent isotopic equilibrium) but did not increase beyond those values. Leu was shown to have a similar behaviour to Ala while Gly behaved similarly to Glu (data not shown).

3.4 | Determination of *n*(AA)

Glu was the AA chosen as anchor for the calculation of the other *n* (AA) values. Data from three different free AA pools and three protein-bound AA pools support this choice. Glu was the AA whose enrichment gradient between extracellular and intracellular free pools was the lowest and showed a consistent ^{2}H elimination rate (k_2) across the free pools. Additionally, protein-bound AA enrichment ratios to BW seemed to reach similar levels to those found in the free pools. The data imply that Glu is the analysed AA which is closer to isotopic equilibrium across the different analysed tissues in our broiler chicken experiment.

The *n*(Glu) value calculated from liver free AA (3.67) was the value chosen as an anchor. As we observed a compartmentation effect on the overall enrichment of free AA, we decided it was best to use a measurement in a pool closer to the site of synthesis and not consider plasma free *n*(Glu) enrichment (3.71). With regards to muscle, muscle free *n*(Glu) (3.36) could have been averaged with the

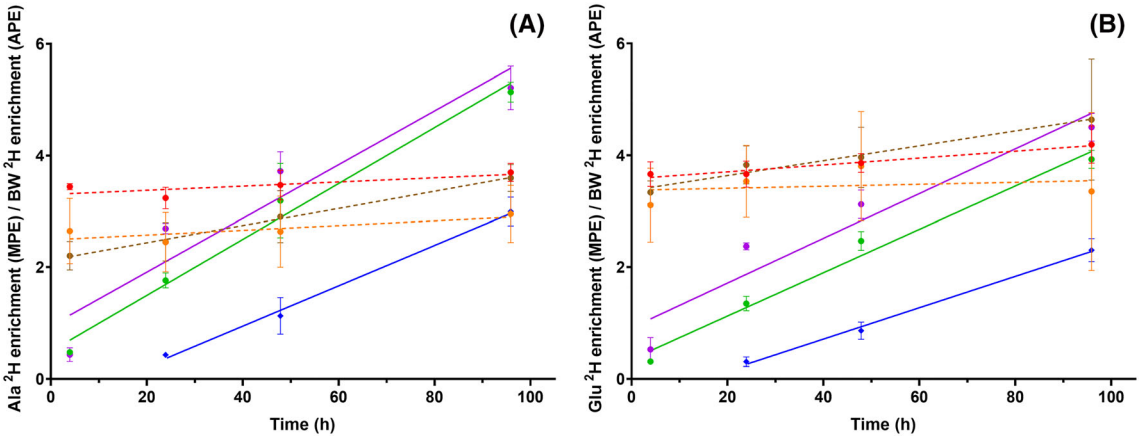

FIGURE 2 Ala/BW (A) and Glu/BW (B) ^{2}H enrichment ratio over time in the plasma free AA pool (red), muscle free AA pool (orange), liver free AA pool (brown), albumin-bound AA pool (green), muscle-bound AA pool (blue) and fibrinogen-bound AA pool (purple). Each data point represents the mean ± SD of five independent measurements, each of them collected from one of the analysed pens. [Color figure can be viewed at wileyonlinelibrary.com]

liver derived value in order to obtain an average tissue *n*(Glu) but as the muscle free AA dataset was weaker and less precise, liver derived *n*(Glu) appeared the better choice.

Different AA enrichment ratios to Glu in the three analysed protein-bound pools were averaged in order to obtain the ratio that would be used for *n*(AA) calculation. Ratios were determined for Gly, Ala, Pro, Val, Leu, Ile and Phe. The methods used in this study did not make the determination of other AA enrichment ratios from experimental data for various reasons: imprecise measurement at low enrichment (Met, Lys, Trp and Tyr); poor derivatization yield (Ser, Thr); heavy fragmentation in the MS ion source (His); oxidation during processing (Cys), Arg reacts but does not form a volatile derivative using the chosen reagents; Asn/Asp enrichment data being combined as a result of acid hydrolysis. Ratios for these AAs were determined from an available literature *n*(AA) table. The reference literature *n* (AA) table has conventionally been the one obtained from Commerford et al, data using tritiated water in mice.[57] The use of this table in modern dynamic proteomics studies has been supported by its close correlation with the direct measurement of plasma free AA enrichment.[39] However, it was decided to use the more recent *n* (AA) table of Ilchenko and co-workers as a reference as this was produced with the original aim of being used in dynamic proteomics studies and used the most recent technology available.[40] Therefore, missing AA enrichment ratios were calculated as the ratio between *n* (Glu) and the appropriate AA *n* in the *n*(AA) table of Ilchenko and co-workers.

The resulting *n*(AA) table (Table 1) shows two values which could be considered above theory. Reported *n*(Ala) is 4.59 while Ala can only incorporate four ^{2}H atoms into its structure; similarly, reported *n* (Leu) is 1.3 when, as an essential AA, it should not incorporate more than one ^{2}H atom. However, *n* is defined as the apparent number of ^{2}H atoms incorporated into an AA and is derived from the relation between BW and aminoacyl t-RNA ^{2}H enrichment. As a result, these *n*(AA) values might be reflecting other phenomena affecting the precursor pool such as tracer recycling, compartmentation effects, kinetic delays or a combination.

TABLE 1 Calculated broiler chicken *n*(AA).

Name	Three-letter code	*n*(AA)
Glutamine	Gln	3.67
Asparagine	Asn	0.69
Serine	Ser	1.61
Glycine	Gly	1.34
Threonine	Thr	0.10
Alanine	Ala	4.59
Aspartic acid	Asp	2.55
Proline	Pro	0.57
Methionine	Met	1.02
Valine	Val	0.78
Glutamic acid	Glu	3.67
Histidine	His	1.40
Lysine	Lys	0.12
Leucine	Leu	1.30
Isoleucine	Ile	0.76
Phenylalanine	Phe	0.84
Cysteine	Cys	1.53
Tyrosine	Tyr	0.75
Arginine	Arg	1.36
Tryptophan	Trp	0.00

Values of *n*(pep) calculated for four different peptides (TCVADENAENCDK, SIHTLFGDK, LVQEVTDFAK, FPNAEFAEITK) using the calculated *n*(AA) table were compared with *n*(pep) values calculated using *n*(AA) values from the two literature tables previously

mentioned. On average, calculated *n*(pep) values were 15% higher than the ones obtained from Ilchenko data and 4% lower than the ones obtained from Commerford data.

3.5 | Broiler chicken FSR

Broiler chicken albumin FSR, MMP FSR and fibrinogen FSR were calculated using Equation (6) for the different pens from which protein-bound AA data had been collected using protein-bound Glu ^2H enrichment and *n*(Glu). Six different albumin, MYHC and fibrinogen peptides identified in the proteomics analysis and manually selected in Skyline as described above had their FSR calculated using Equation (7) (Table 2). Results were in agreement with expected values for these proteins, fibrinogen being the one with the fastest FSR and MMP showing a lower rate of synthesis. These data were not powered to allow any significant claim to be made on the effect of the different experimental variables on protein FSR, but a reduction in albumin FSR and MMP FSR following an immune challenge is coherent with previous reports on albumin being a negative acute phase protein in broiler chicken and growth being compromised under stress conditions.[58]

A Bland–Altman residual plot was created with the aim of comparing protein FSR values calculated using the two different methodologies described in this study (Figure 3).[59] Albumin FSR values calculated from albumin-bound Glu enrichment were compared with the mean albumin peptide FSR value calculated from proteomics data. MMP FSR values calculated from MMP-bound Glu enrichment were compared with the mean MYHC peptide FSR value calculated from proteomics data. Fibrinogen FSR values calculated from fibrinogen-bound Glu enrichment were compared with the mean fibrinogen peptide FSR value calculated from proteomics data. A good agreement was found between the GC/MS method and the dynamic proteomics method with the mean residual value being −4.24% day^{-1} and only one measurement appearing outside the limit of agreement.

Figure 4 shows the regression line that results from the comparison of GC/MS and proteomics FSR calculated values which has a slope of 1.41. Lin's coefficient of concordance (ρ_c), which evaluates how a set of paired values compare to the 45° bisector angle and is an alternative method to evaluate the agreement between measurements, showed a value of 0.865 (95% CI: >0.7594 or <0.9262).[60] This results indicates an excellent agreement as interpreted by Altman (ρ_c > 0.80) although it can also be regarded as a poorer agreement following the interpretation of McBride (lower CI < 0.9).[61,62]

4 | DISCUSSION

A new approach, pairing a single ^2H_2O bolus labelling strategy with dynamic proteomics for the measurement of protein FSR, has been described and validated in this study. This method is especially convenient for its application in animal research and it also offers an economic alternative to other more established methods. Results from this study showed that some common assumptions in the study of protein dynamics may not always be fulfilled, at least in broiler chickens. In order to account for some of the observed phenomena, a novel method for the determination of the pattern of free AA labelling with respect to BW (*n*(AA)) has been developed. Broiler chicken individual protein FSRs have been calculated using two independent approaches, with good agreement between them. The agreement between these methods provides indirect support for the novel method used to estimate *n*(AA).

Not only is the proposed protein labelling methodology convenient for use in farm animals, but the analytical pipeline has also been optimized to allow on-farm measurements of ^2H enrichment by using a portable FTIR spectrometer. However, from an experimental design perspective, the present study has certain limitations which are important to consider. Oral ^2H_2O administration to broiler chickens was performed by using a syringe to drop ^2H_2O into the chicken's beak instead of a gavage device. This decision was made with the aim to minimize chicken stress but resulted in frequent loss of some ^2H_2O making it impossible to control the exact amount of ^2H_2O administered. The equilibration of orally administered ^2H_2O with BW was observed to occur more slowly than in other species of similar body size, such as rodents, or as scaled from body size, in humans or dogs.[41,63] After 1 h, measurements of BW ^2H enrichment showed incomplete BW labelling compared with 4 h (data not shown). Slow oral ^2H_2O equilibration with BW in broiler chickens might be due to fluid hold-up in the crop. This phenomenon may limit the accuracy of estimating fast-turnover protein FSR (FSR ≥ 200% day^{-1}) following oral ^2H_2O administration in chicken. However, timepoints selected in this study aimed to provide data that allowed the calculation of a wide range of protein FSRs without particularly targeting fast or slow proteins. Muscle protein FSR was estimated using data collected at four different timepoints due to the low ^2H enrichment found in the 4 h samples; a selection of later sampling timepoints may have improved the accuracy of these estimates. Contrarily, estimates of fast-turnover protein FSR would have benefitted from an increased number of sampling points in the early stages of the labelling period. Careful experimental design is key for an accurate calculation of protein FSR. Further studies using ^2H_2O in farm animals would require appropriate planning and pilot experiments that allow informed decisions about experimental design from a physiological and practical perspective. It should be noted that studies on larger animals would allow repeated blood sampling from the same individuals and the calculation of plasma protein FSR at an individual animal level.

Results from this study suggest that assumptions made by us and others, relating to a simple precursor pool, may not be representative of the detailed biology. Results from early mammalian studies using ^2H_2O labelling observed that ^2H_2O equilibrates rapidly with BW and labels free AA pools across all cellular compartments.[31–33,35,38] This fast equilibration would eliminate inconveniences related with the use of labelled AAs as isotopic tracers such as true precursor determination or tracer recycling and would allow the use of plasma

TABLE 2 (A) On the left, six albumin peptide FSRs (% day^{-1}) calculated using Equation (7) and mean ± standard deviation (STD). On the right, albumin FSR (% day^{-1}) calculated using Equation (6). When B = Glu enrichment and n(AA) = n(Glu). (B) On the left, six MYHC peptide FSRs (% day^{-1}) calculated using Equation (7) and mean ± STD. On the right, MMP FSR (% day^{-1}) calculated using Equation (6). When B = Glu enrichment and n(AA) = n(Glu). (C) On the left, three fibrinogen alpha subunit (VISGPDGPREEIVEK, SFDYQVDKEGYDNIQK and MVSSDGSDC[CAM]SHLQGGR), one fibrinogen beta subunit (QDGSVNFGR) and two fibrinogen gamma subunit (TIYPSEK and GTADYAVFK) peptide FSRs (% day^{-1}) calculated using Equation (7) and mean ± STD. On the right, fibrinogen FSR (% day^{-1}) calculated using Equation (6). When B = Glu enrichment and n(AA) = n(Glu).

A	YVPPPFNPDMFSFDEK	PQMTEEQIK	MPQVPTDLLLETGK	PADLPSLVEK	DVVDLAQK	APFSEVSK	Mean ± STD	Albumin FSR
Unchallenged	45.27	69.36	52.15	55.01	58.09	68.72	58.1 ± 9.5	55.75
Challenged	32.97	43.03	37.85	40.10	40.48	45.60	40 ± 4.4	47.94
Control diet	32.29	46.83	38.61	40.75	38.99	49.46	41.2 ± 6.2	61.25
Diet 1	29.62	43.19	35.40	41.47	40.97	40.74	38.6 ± 5.1	60.47
Diet 2	33.21	48.42	34.79	39.91	39.28	45.26	40.2 ± 5.9	51.75
B	**QAEEAEELSNVNLSK**	**LTGAVMHYGNLK**	**PMGIFSILEEEC (CAM)MFPK**	**LQTESGEYSRQVEEK**	**AITDAAMMAEELK**	**DALISQLSR**	**Mean ± STD**	**MMP FSR**
Unchallenged	16.57	16.86	17.05	9.06	16.63	15.16	15.23 ± 3.1	15.73
Challenged	11.56	10.74	15.33	11.96	11.30	21.06	13.66 ± 4	11.96
Control diet	16.53	15.07	13.91	10.34	13.50	17.27	14.44 ± 2.5	18.36
Diet 1	13.10	9.72	13.73	8.36	12.80	14.81	12.09 ± 2.5	13.92
Diet 2	16.07	14.82	14.73	10.43	12.47	15.72	14.04 ± 2.2	13.93
C	**VISGPDGPREEIVEK**	**SFDYQVDKEGYDNIQK**	**MVSSDGSDC (CAM)SHLQGGR**	**QDGSVNFGR**	**TIYPSEK**	**GTADYAVFK**	**Mean ± STD**	**Fibrinogen FSR**
Control diet	120.42	123.69	157.85	180.89	98.75	127.70	134.9 ± 29.4	98.20
Diet 1	124.20	96.77	154.49	143.05	100.64	104.05	120.53 ± 24.1	94.36
Diet 2	153.75	151.54	152.28	173.84	185.84	163.16	163.4 ± 13.9	107.65

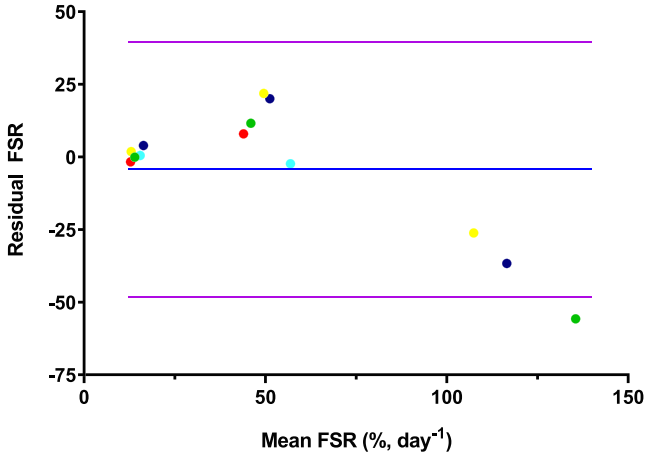

FIGURE 3 Bland–Altman residual plot comparing FSR values calculated using the two different methods described in this study. In the *X* axis, the mean between two independent measurements of FSR is represented. On the *Y* axis, residual FSR calculated by subtracting the proteomics FSR estimate from the protein-bound AA derived FSR estimate is represented. Blue line represents the mean residual value (*d*) across all measurements ($n = 13$). Purple lines represent the limits of agreement, calculated as $d \pm 2 \times$ residual standard deviation. Dot colours: light blue = unchallenged; red = challenged; dark blue = control diet; yellow = diet 1; green = diet 2. [Color figure can be viewed at wileyonlinelibrary.com]

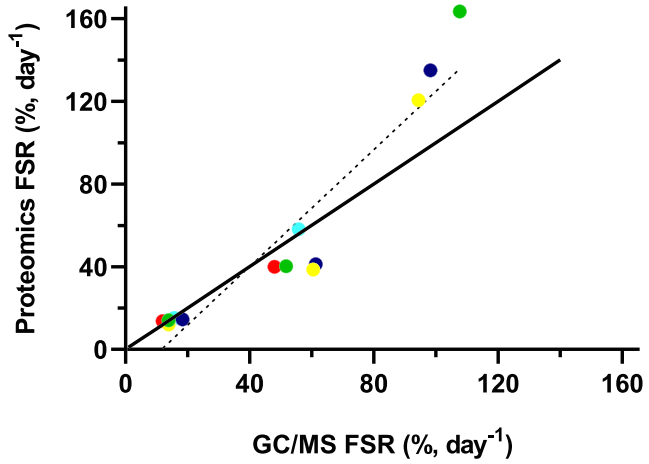

FIGURE 4 GC/MS calculated FSR values (*X* axis) against proteomics calculated FSR values (*Y* axis). Solid line represents the 45° line of no difference to which values are compared by Lin's concordance correlation coefficient. Discontinuous line represents the regression line of calculated FSR values. Dot colours: light blue = unchallenged; red = challenged; dark blue = control diet; yellow = diet 1; green = diet 2. [Color figure can be viewed at wileyonlinelibrary.com]

free AA enrichment as a proxy for aminoacyl t-RNA enrichment. The observation of different AA ^{2}H elimination rates compared to BW in different cellular compartments and increased ^{2}H enrichment at the site of protein synthesis for some AAs could be explained by compartmentation and tracer recycling phenomena which would imply that, while the use of ^2H_2O alleviates the impact of these metabolic phenomena in protein FSR calculation, it does not eliminate them, so they should still be taken into consideration for the most accurate FSR estimation. However, observed results may be exclusive to the broiler chicken model and not fully extrapolated to mammalian species. The fact that Ala and Leu were the two AAs for which ^{2}H at the site of synthesis seemed to be the highest compared with the analysed free AA pools contrasts with previous studies on Ala enrichment, whose ^{2}H labelling has been the most extensively studied.[31,33,38] Chickens consume starchy diets and have higher and more variable plasma glucose concentrations than mammals, which have tighter insulin control.[64] High glucose promotes a high glycolytic flux with the resulting pyruvic acid production, which on transamination, forms Ala. A high pyruvate flux may disturb the labelling pattern from BW in comparison to mammals. The intracellular site of protein breakdown, *de novo* AA synthesis and site of protein synthesis may be influenced by compartmentation with the potential for varying Ala enrichment in different compartments. The case of Leu is more difficult to explain from simply a broiler chicken perspective but studies using labelled AAs have reported Leu and other indispensable AAs are more prone to tracer recycling where intracellular free enrichment increases with time as their concentration, unlike dispensable AAs, is not elevated relative to the extracellular free AA pool.[65,66] As well as low enrichment in some fast-turnover pools, this phenomenon may cause enrichment to increase with time due to re-entry of tracer into the free pool (recycling). The effect could have been amplified by the single-bolus ^2H_2O labelling experimental design although a plateau labelling experimental design is fundamentally a series of ^2H_2O boli and should therefore show a similar pattern. Briefer measurement periods will reduce this phenomenon in either case. It would seem prudent to limit the measurement period in future uses of the single-bolus D_2O dose to one tracer elimination half-time (*ca* 48 hours in 1 kg chicken) rather than two, as is feasible when simply considering the tracer enrichments observed. It would be of interest to confirm the protein-bound AA ^{2}H labelling pattern established in this study while following an extended plateau labelling protocol so that a comparison of bound AA ^{2}H enrichment ratios could be performed.

The observations related to differential ^{2}H AA labelling across free pools motivated the calculation of an *n*(AA) table specific for our experiments. The method as applied was informed by studies in which *n*(AA) values have been derived from peptide enrichment data but made use of available protein-bound AA enrichment ratios instead.[37,39,40] Our *n*(AA) calculation was limited by the modest tracer levels used and the AA enrichment analysis pipeline chosen, which needed to be complemented by literature data in order to obtain AA enrichment ratios relative to Glu for all AAs. The resulting *n*(AA) table showed values comparable to those available in the literature and produced *n*(pep) values that were, on average, between the results obtained by using other reference tables. It is important to highlight that calculated *n*(Ala) and *n*(Leu) values were higher than the

theoretical amount of ^{2}H atoms that can be incorporated into the AA structure. These values are the result of the phenomena that have been described in the previous paragraph and an accurate estimation of the apparent ^{2}H labelling of those AAs at the site of protein synthesis. Results obtained for *n*(Pro) are consistent with the finding of Ilchenko et al and notably lower than those obtained by Commerford et al and applied by Price et al. These results are coherent with reports on humans and broiler chickens on Pro being derived from the diet and suggesting that a low rate of *de novo* synthesis is normal in an adequate diet.[41,67,68] The case of Pro may be an example of technical limitations present in the pioneering work of Commerford et al that may have led to an overestimation of Pro enrichment due to an incomplete separation from Glu during the cation exchange procedure as applied. Similar to the analysis performed in this study, the Commerford method was not capable of discriminating between Asp and Asn which was proven important by the results of Ilchenko et al. These examples support our choice of using the Ilchenko et al data to derive the enrichment ratios of missing AA to Glu. It is worth noting that none of the aforementioned *n*(AA) tables is likely to be completely accurate. AA labelling at the site of synthesis is a dynamic phenomenon that would likely be different for different species, tissues and metabolic states as has been previously observed.[35,40] A compromise must be reached between FSR calculation accuracy and practicality of the analysis. Reported *n*(AA) values in this study have been calculated by pooling data from broiler chickens undergoing different experimental conditions and with more than likely individual differences in AA metabolism. However, these values are more representative of broiler chicken AA metabolism and the experimental conditions in the present study than other (mammalian) *n*(AA) values in the literature as well as a good foundation for comparative studies of broiler chicken individual protein FSR calculated from proteomics data.

Reported broiler chicken FSR values in this study are the first calculated following a $^{2}H_2O$ labelling approach. Mixed breast muscle protein FSR values for growing broiler chicken (21 days old) are in line with most values previously reported in the literature where FSR ranges between 10% day^{-1} and 30% day^{-1}.[11,13–15,18,69,70] However, recent studies performed by Maharjan and co-workers have reported higher FSR values, around 35% day^{-1}.[22,23,29] The observed increase in breast muscle FSR was attributed to the improved genetics of modern broiler chicken lines. Differences in tracer model, diet composition, genetic lines or developmental stage (21–25 days as opposed to 21 days) could contribute towards the disparity found between the reported values here and those reported by Maharjan et al. Values for broiler chicken albumin and fibrinogen FSR have not been previously reported in the literature although values of 31.2/44.8%, 91%, 110.4%, 114.4% and 176% FSR per day have been reported for mixed liver proteins.[12–15,24] Reported FSR values in this study calculated using two different analytical approaches show good agreement; however, this comparison has certain limitations: (a) isolated albumin was not completely pure which could limit the accuracy of the GC/MS-derived albumin FSR estimates; (b) MMP FSR was compared with MYHC FSR because it is the most abundant protein in muscle tissue and the one that would contribute the most towards MMP FSR; (c) the use of an unequal number of fibrinogen peptides from different subunits for FSR calculation resulted from the fact that they were the only acceptable fibrinogen peptides (according to the described selection criteria) present across the 15 analysed samples; and (d) the fact that two different proteomics platforms, whose accuracy for measuring mass isotopologue intensities might not be equal, were used for the calculation of dynamic proteomics FSR. Furthermore, the accuracy of faster FSR values may have been compromised by slow tracer equilibration and limited early sampling points. Overall agreement between FSR estimates validate the assumptions used with respect to the precursor pool for protein synthesis and the use of the proposed dynamic proteomics approach for the measurement of individual broiler protein FSR.

A new methodology for the calculation of individual protein FSR has been developed and validated in this study. This methodology offers an economic advantage when compared to other strategies and is especially convenient for its use on free-living animals. Implementation of this approach on larger animals, allowing repeated blood sampling from the same individual, would reduce the variability of the precursor term and improve the reliability of FSR estimations. This methodology could help in expanding dynamic proteomics studies to farm animals, helping to better characterize growth and immunity metabolism as well as assessing the effect of different experimental variables, which could in turn result in the characterization of novel biomarkers and contribute towards healthier and more profitable livestock systems.

ACKNOWLEDGMENTS

The authors would like to thank the European Commission for funding the present study as part of the European Union's Horizon 2020 research and innovation programme 2020-MSCA-ITN-2017-EJD under the Marie Skłodowska-Curie Innovative Training Networks (European Joint Doctorate in Molecular Animal Nutrition, MANNA), grant agreement no. 765423. The authors are grateful for the additional funding from the EPIC-XS project number 823839, funded by the Horizon 2020 programme of the European Union. The authors would like to thank Geert Bruggeman and David Hermans from Nuscience for designing and providing the chicken diets that were used in this study as well as Dr Andrej Kovác and Dr Petra Majerová from the Institute of Neuroimmunology in Slovakia for support in the proteomic analysis of part of the samples included in this study, Dr Chris Chadwick from Life Diagnostics for advice as industrial supervisor, Professor David Eckersall from the University of Glasgow as the main coordinator of the MANNA-ITN and Dr Alexander Corbishley from the University of Edinburgh for his support in the analysis of the data.

DATA AVAILABILITY STATEMENT

The data that support the findings of this study are available from the corresponding author upon reasonable request.

ORCID

Jorge Peinado-Izaguerri https://orcid.org/0000-0002-6607-8295

PEER REVIEW

The peer review history for this article is available at https://www.webofscience.com/api/gateway/wos/peer-review/10.1002/rcm.9497.

REFERENCES

1. Ohsumi Y. Protein turnover. *IUBMB Life*. 2006;58(5-6):363-369. doi:10.1080/15216540600758539
2. Lau E, Cao Q, Ng DCM, et al. A large dataset of protein dynamics in the mammalian heart proteome. *Sci Data*. 2016;3(1):160015. doi:10.1038/sdata.2016.15
3. Ross AB, Langer JD, Jovanovic M. Proteome turnover in the spotlight: Approaches, applications, and perspectives. *Mol Cell Proteomics*. 2021;20:100016. doi:10.1074/mcp.R120.002190
4. Doherty MK, Beynon RJ. Protein turnover on the scale of the proteome. *Expert Rev Proteomics*. 2006;3(1):97-110. doi:10.1586/14789450.3.1.97
5. Smail MA, Reigle JK, McCullumsmith RE. Using protein turnover to expand the applications of transcriptomics. *Sci Rep*. 2021;11(1):4403. doi:10.1038/s41598-021-83886-7
6. Schwanhäusser B, Busse D, Li N, et al. Global quantification of mammalian gene expression control. *Nature*. 2011;473(7347):337-342. doi:10.1038/nature10098
7. Hellerstein M, Evans W. Recent advances for measurement of protein synthesis rates, use of the 'virtual biopsy' approach, and measurement of muscle mass. *Curr Opin Clin Nutr Metab Care*. 2017;20(3):191-200. doi:10.1097/MCO.0000000000000370
8. OECD and FAO of the UN. OECD-FAO agricultural outlook 2022-2031. Published online 2022. Accessed September 9, 2022. https://www.oecd-ilibrary.org/content/publication/f1b0b29c-en
9. Maruyama K, Sunde M, Swick R. Growth and muscle protein turnover in the chick. *Biochem J*. 1978;176(2):573-582. doi:10.1042/bj1760573
10. Maeda Y, Hayashi K, Toyohara S, Hashiguchi T. Variation among chicken stocks in the fractional rates of muscle protein synthesis and degradation. *Biochem Genet*. 1984;22(7–8):687-700. doi:10.1007/BF00485853
11. Muramatsu T, Okumura J. Whole-body protein turnover in chicks at early stages of growth. *J Nutr*. 1985;115(4):483-490. doi:10.1093/jn/115.4.483
12. Hiramoto K, Muramatsu T, Okumura J. Protein synthesis in tissues and in the whole body of laying hens during egg formation. *Poult Sci*. 1990;69(2):264-269. doi:10.3382/ps.0690264
13. Jones SJ. Improvement of growth in broiler chickens using trilostane. *Poult Sci*. 1990;69(12):2143-2149. doi:10.3382/ps.0692143
14. Nieto R, Palmer RM, Fernández-Fígares I, Pérez L, Prieto C. Effect of dietary protein quality, feed restriction and short-term fasting on protein synthesis and turnover in tissues of the growing chicken. *Br J Nutr*. 1994;72(4):499-507. doi:10.1079/bjn19940054
15. Tesseraud S, Peresson R, Lopes J, Chagneau AM. Dietary lysine deficiency greatly affects muscle and liver protein turnover in growing chickens. *Br J Nutr*. 1996;75(6):853-865. doi:10.1079/bjn19960191
16. Tesseraud S, Chagneau AM, Grizard J. Muscle protein turnover during early development in chickens divergently selected for growth rate. *Poult Sci*. 2000;79(10):1465-1471. doi:10.1093/ps/79.10.1465
17. Dänicke S, Böttcher W, Simon O, Jeroch H. The measurement of muscle protein synthesis in broilers with a flooding dose technique: Use of ^{15}N-labelled phenylalanine, GC-MS and GC-C-IRMS. *Isotopes Environ Health Stud*. 2001;37(3):213-225. doi:10.1080/10256010108033297
18. Urdaneta-Rincon M, Leeson S. Muscle (pectoralis major) protein turnover in young broiler chickens fed graded levels of lysine and crude protein. *Poult Sci*. 2004;83(11):1897-1903. doi:10.1093/ps/83.11.1897
19. Ekmay RD, Salas C, England J, Cerrate S, Coon CN. The effects of age, energy and protein intake on protein turnover and the expression of proteolysis-related genes in the broiler breeder hen. *Comp Biochem Physiol B Biochem Mol Biol*. 2013;164(1):38-43. doi:10.1016/j.cbpb.2012.10.002
20. Vignale K, Caldas JV, England JA, et al. Effect of white striping myopathy on breast muscle (pectoralis major) protein turnover and gene expression in broilers. *Poult Sci*. 2017;96(4):886-893. doi:10.3382/ps/pew315
21. Yuan C, Bu XC, Yan HX, Lu JJ, Zou XT. Dietary L-arginine levels affect the liver protein turnover and alter the expression of genes related to protein synthesis and proteolysis of laying hens. *Poult Sci*. 2016;95(2):261-267. doi:10.3382/ps/pev314
22. Maharjan P, Mullenix G, Hilton K, et al. Effects of dietary amino acid levels and ambient temperature on mixed muscle protein turnover in pectoralis major during finisher feeding period in two broiler lines. *J Anim Physiol Anim Nutr (Berl)*. 2020;104(5):1351-1364. doi:10.1111/jpn.13363
23. Maharjan P, Mullenix G, Hilton K, et al. Effects of dietary energy levels on pectoralis major mixed muscle protein turnover and body composition in two broiler lines housed in different grow-out environments. *J Anim Physiol Anim Nutr (Berl)*. 2021;105(3):535-548. doi:10.1111/jpn.13467
24. Barnes DM, Song Z, Klasing KC, Bottje W. Protein metabolism during an acute phase response in chickens. *Amino Acids*. 2002;22(1):15-26. doi:10.1007/s726-002-8198-6
25. Doherty MK, Whitehead C, McCormack H, Gaskell SJ, Beynon RJ. Proteome dynamics in complex organisms: Using stable isotopes to monitor individual protein turnover rates. *Proteomics*. 2005;5(2):522-533. doi:10.1002/pmic.200400959
26. Kidd MT, Peebles ED, Whitmarsh SK, Yeatman JB, Wideman RF. Growth and immunity of broiler chicks as affected by dietary arginine. *Poult Sci*. 2001;80(11):1535-1542. doi:10.1093/ps/80.11.1535
27. Jones SJ, Aberle ED, Judge MD. Skeletal muscle protein turnover in broiler and layer chicks. *J Anim Sci*. 1986;62(6):1576-1583. doi:10.2527/jas1986.6261576x
28. Vignale K, Caldas JV, England JA, et al. The effect of four different feeding regimens from rearing period to sexual maturity on breast muscle protein turnover in broiler breeder parent stock. *Poult Sci*. 2017;96(5):1219-1227. doi:10.3382/ps/pew369
29. Maharjan P, Weil J, Beitia A, et al. In vivo collagen and mixed muscle protein turnover in 2 meat-type broiler strains in relation to woody breast myopathy. *Poult Sci*. 2020;99(10):5055-5064. doi:10.1016/j.psj.2020.06.059
30. Kasumov T, Willard B, Li L, Sadygov RG, Previs S. Proteome dynamics with heavy water: Instrumentations, data analysis, and biological applications. In: *Recent Advances in Proteomics Research*. IntechOpen; 2015. doi:10.5772/61776
31. Previs SF, Fatica R, Chandramouli V, Alexander JC, Brunengraber H, Landau BR. Quantifying rates of protein synthesis in humans by use of $^{2}H_2O$: Application to patients with end-stage renal disease. *Am J Physiol Endocrinol Metab*. 2004;286(4):E665-E672. doi:10.1152/ajpendo.00271.2003
32. Dufner DA, Bederman IR, Brunengraber DZ, et al. Using $^{2}H_2O$ to study the influence of feeding on protein synthesis: Effect of isotope equilibration in vivo vs. in cell culture. *Am J Physiol Endocrinol Metab*. 2005;288(6):E1277-E1283. doi:10.1152/ajpendo.00580.2004

33. Busch R, Kim YK, Neese RA, et al. Measurement of protein turnover rates by heavy water labeling of nonessential amino acids. *Biochim Biophys Acta*. 2006;1760(5):730-744. doi:10.1016/j.bbagen.2005.12.023
34. Cabral CB, Bullock KH, Bischoff DJ, Tompkins RG, Yu YM, Kelleher JK. Estimating glutathione synthesis with deuterated water: A model for peptide biosynthesis. *Anal Biochem*. 2008;379(1):40-44. doi:10.1016/j.ab.2008.04.042
35. Rachdaoui N, Austin L, Kramer E, et al. Measuring proteome dynamics in vivo: As easy as adding water? *Mol Cell Proteomics*. 2009;8(12):2653-2663. doi:10.1074/mcp.M900026-MCP200
36. Li L, Willard B, Rachdaoui N, et al. Plasma proteome dynamics: Analysis of lipoproteins and acute phase response proteins with $^{2}H_2O$ metabolic labeling. *Mol Cell Proteomics*. 2012;11(7):M111.014209. doi:10.1074/mcp.M111.014209
37. Kasumov T, Ilchenko S, Li L, et al. Measuring protein synthesis using metabolic ^{2}H labeling, high-resolution mass spectrometry, and an algorithm. *Anal Biochem*. 2011;412(1):47-55. doi:10.1016/j.ab.2011.01.021
38. Belloto E, Diraison F, Basset A, Allain G, Abdallah P, Beylot M. Determination of protein replacement rates by deuterated water: Validation of underlying assumptions. *Am J Physiol Endocrinol Metab*. 2007;292(5):E1340-E1347. doi:10.1152/ajpendo.00488.2006
39. Price JC, Holmes WE, Li KW, et al. Measurement of human plasma proteome dynamics with $^{2}H_2O$ and liquid chromatography tandem mass spectrometry. *Anal Biochem*. 2012;420(1):73-83. doi:10.1016/j.ab.2011.09.007
40. Ilchenko S, Haddad A, Sadana P, Recchia FA, Sadygov RG, Kasumov T. Calculation of the protein turnover rate using the number of incorporated ^{2}H atoms and proteomics analysis of a single labeled sample. *Anal Chem*. 2019;91(22):14340-14351. doi:10.1021/acs.analchem.9b02757
41. MacDonald AJ, Small AC, Greig CA, et al. A novel oral tracer procedure for measurement of habitual myofibrillar protein synthesis. *Rapid Commun Mass Spectrom*. 2013;27(15):1769-1777. doi:10.1002/rcm.6622
42. Wilkinson DJ, Franchi MV, Brook MS, et al. A validation of the application of D_2O stable isotope tracer techniques for monitoring day-to-day changes in muscle protein subfraction synthesis in humans. *Am J Physiol Endocrinol Metab*. 2014;306(5):E571-E579. doi:10.1152/ajpendo.00650.2013
43. MacDonald AJ, Johns N, Stephens N, et al. Habitual myofibrillar protein synthesis is normal in patients with upper GI cancer cachexia. *Clin Cancer Res*. 2015;21(7):1734-1740. doi:10.1158/1078-0432.CCR-14-2004
44. IAEA. Assessment of body composition and total energy expenditure in humans using stable isotope techniques. International Atomic Energy Agency; 2009. Accessed September 9, 2022. https://www.iaea.org/publications/7982/assessment-of-body-composition-and-total-energy-expenditure-in-humans-using-stable-isotope-techniques
45. Jennings G, Bluck L, Wright A, Elia M. The use of infrared spectrophotometry for measuring body water spaces. *Clin Chem*. 1999;45(7):1077-1081. doi:10.1093/clinchem/45.7.1077
46. Takeda Y. Studies of the metabolism and distribution of fibrinogen in healthy men with autologous 125-I-labeled fibrinogen. *J Clin Invest*. 1966;45(1):103-111. doi:10.1172/JCI105314
47. Svagera Z, Hanzlíková D, Simek P, Hušek P. Study of disulfide reduction and alkyl chloroformate derivatization of plasma sulfur amino acids using gas chromatography-mass spectrometry. *Anal Bioanal Chem*. 2012;402(9):2953-2963. doi:10.1007/s00216-012-5727-y
48. Korner A, Debro JR. Solubility of albumin in alcohol after precipitation by trichloroacetic acid: A simplified procedure for separation of albumin. *Nature*. 1956;178(4541):1067. doi:10.1038/1781067a0
49. Montigon F, Boza JJ, Fay LB. Determination of ^{13}C- and ^{15}N-enrichment of glutamine by gas chromatography/mass spectrometry and gas chromatography/combustion/isotope ratio mass spectrometry after N(O,S)-ethoxycarbonyl ethyl ester derivatisation. *Rapid Commun Mass Spectrom*. 2001;15(2):116-123. doi:10.1002/1097-0231(20010130)15:2%3C116::AID-RCM202%3E3.0.CO;2-3
50. Huang ZH, Wang J, Gage DA, Watson JT, Sweeley CC, Husek P. Characterization of N-ethoxycarbonyl ethyl esters of amino acids by mass spectrometry. *J Chromatogr*. 1993;635(2):271-281. doi:10.1016/0021-9673(93)80370-n
51. Almeida AM, Nanni P, Ferreira AM, et al. The longissimus thoracis muscle proteome in Alentejana bulls as affected by growth path. *J Proteomics*. 2017;152:206-215. doi:10.1016/j.jprot.2016.10.020
52. Hughes CS, Moggridge S, Müller T, Sorensen PH, Morin GB, Krijgsveld J. Single-pot, solid-phase-enhanced sample preparation for proteomics experiments. *Nat Protoc*. 2019;14(1):68-85. doi:10.1038/s41596-018-0082-x
53. Cox J, Neuhauser N, Michalski A, Scheltema RA, Olsen JV, Mann M. Andromeda: A peptide search engine integrated into the MaxQuant environment. *J Proteome Res*. 2011;10(4):1794-1805. doi:10.1021/pr101065j
54. Dorfer V, Pichler P, Stranzl T, et al. MS Amanda, a universal identification algorithm optimized for high accuracy tandem mass spectra. *J Proteome Res*. 2014;13(8):3679-3684. doi:10.1021/pr500202e
55. Pino LK, Searle BC, Bollinger JG. The Skyline ecosystem: Informatics for quantitative mass spectrometry proteomics. *Mass Spectrom Rev*. 2020;39(3):229-244. doi:10.1002/mas.21540
56. Cardinali B, Profumo A, Aprile A, et al. Hydrodynamic and mass spectrometry analysis of nearly-intact human fibrinogen, chicken fibrinogen, and of a substantially monodisperse human fibrinogen fragment X. *Arch Biochem Biophys*. 2010;493(2):157-168. doi:10.1016/j.abb.2009.10.008
57. Commerford SL, Carsten AL, Cronkite EP. The distribution of tritium among the amino acids of proteins obtained from mice exposed to tritiated water. *Radiat Res*. 1983;94(1):151-155. doi:10.2307/3575870
58. Adler KL, Peng PH, Peng RK, Klasing KC. The kinetics of hemopexin and alpha1-acid glycoprotein levels induced by injection of inflammatory agents in chickens. *Avian Dis*. 2001;45(2):289-296. doi:10.2307/1592967
59. Bland JM, Altman DG. Statistical methods for assessing agreement between two methods of clinical measurement. *Lancet*. 1986;1(8476):307-310.
60. Lin LI. A concordance correlation coefficient to evaluate reproducibility. *Biometrics*. 1989;45(1):255-268. doi:10.2307/2532051
61. Altman DG. *Practical Statistics for Medical Research*. Chapman and Hall/CRC; 1990. doi:10.1201/9780429258589
62. McBride B. A proposal for strength-of-agreement criteria for Lin's concordance. Published online 2005.
63. Gabisonia K, Burjanadze G, Woitek F, et al. Proteome dynamics and bioinformatics reveal major alterations in the turnover rate of functionally related cardiac and plasma proteins in a dog model of congestive heart failure. *J Card Fail*. 2022;28(4):588-600. doi:10.1016/j.cardfail.2021.11.011
64. Koochaksaraie R, Irani M, Valizadeh M, Rahmani Z, Gharahveysi S. A study on the effect of cinnamon powder in diet on serum glucose level in broiler chicks. *Global Veterinaria*. 2010;4:562-565.
65. Davies DD, Humphrey TJ. Amino acid recycling in relation to protein turnover. *Plant Physiol*. 1978;61(1):54-58. doi:10.1104/pp.61.1.54
66. Wagenmakers AJ. Tracers to investigate protein and amino acid metabolism in human subjects. *Proc Nutr Soc*. 1999;58(4):987-1000. doi:10.1017/s0029665199001305

67. Jim S, Jones V, Ambrose SH, Evershed RP. Quantifying dietary macronutrient sources of carbon for bone collagen biosynthesis using natural abundance stable carbon isotope analysis. *Br J Nutr*. 2006; 95(6):1055-1062. doi:10.1079/bjn20051685
68. Berthold HK, Hachey DL, Reeds PJ, Thomas OP, Hoeksema S, Klein PD. Uniformly ^{13}C-labeled algal protein used to determine amino acid essentiality in vivo. *Proc Natl Acad Sci USA*. 1991;88(18): 8091-8095. doi:10.1073/pnas.88.18.8091
69. Hayashi K, Tomita Y, Maeda Y, Shinagawa Y, Inoue K, Hashizume T. The rate of degradation of myofibrillar proteins of skeletal muscle in broiler and layer chickens estimated by N tau-methylhistidine in excreta. *Br J Nutr*. 1985;54(1):157-163. doi:10.1079/bjn19850101
70. Jones SJ, Judge MD, Aberle ED. Muscle protein turnover in sex-linked dwarf and normal broiler chickens. *Poult Sci*. 1986;65(11): 2082-2089. doi:10.3382/ps.0652082

SUPPORTING INFORMATION

Additional supporting information can be found online in the Supporting Information section at the end of this article.

How to cite this article: Peinado-Izaguerri J, Zarzuela E, McLaughlin M, et al. A novel dynamic proteomics approach for the measurement of broiler chicken protein fractional synthesis rate. *Rapid Commun Mass Spectrom*. 2023;37(10): e9497. doi:10.1002/rcm.9497